J Mater Sci: Mater Med (2018) 29:17
DOI 10.1007/s10856-017-6017-1

CLINICAL APPLICATIONS OF BIOMATERIALS

Original Research

Osteoinduction and -conduction through absorbable bone substitute materials based on calcium sulfate: in vivo biological behavior in a rabbit model

D. Pförringer[1] · N. Harrasser[2] · H. Mühlhofer[2] · M. Kiokekli[2] · A. Stemberger[2] · M. van Griensven[1] · M. Lucke[3] · R. Burgkart[2] · A. Obermeier[2]

Received: 7 October 2017 / Accepted: 5 December 2017 / Published online 9 January 2018

Abstract Calcium sulfate (CS) can be used as an antibiotically impregnated bone substitute in a variety of clinical constellations. Antibiotically loaded bone substitutes find specific application in orthopedic and trauma surgery to prevent or treat bone infections especially in relation to open bone defects. However, its use as a structural bone graft reveals some concerns due to its fast biodegradation. The addition of calcium carbonate and tripalmitin makes CS formulations more resistant to resorption leaving bone time to form during a prolonged degradation process. The aim of the present study was the evaluation of biocompatibility and degradation properties of newly formulated antibiotically impregnated CS preparations. Three different types of CS bone substitute beads were implanted into the tibial metaphysis of rabbits (CS dihydrate with tripalmitin, containing gentamicin (Group A) or vancomycin (Group B); Group C: tobramycin-loaded CS hemihydrate). Examinations were performed by means of x-ray, micro-computed tomography (micro-CT) and histology after 4, 6, 8 and 12 weeks. Regarding biocompatibility of the formulations, no adverse reactions were observed. Histology showed formation of vital bone cells attached directly to the implanted materials, while no cytotoxic effect in the surrounding of the beads was detected. All CS preparations showed osteogenesis associated to implanted material. Osteoblasts attached directly to the implant surface and revealed osteoid production, osteocytes were found in newly mineralized bone. Group C implants (Osteoset®) were subject to quick degradation within 4 weeks, after 6–8 weeks there were only minor remnants with little osteogenesis demonstrated by histological investigations. Group A implants (Herafill®-G) revealed similar degradation within atleast 12 weeks. In contrast, group B implants (CaSO4-V) were still detectable after 12 weeks with the presence of implant-associated osteogenesis atlatest follow-up. In all of these preparations, giant cells were found during implant degradation on surface and inside of resorption lacunae. None of the analyzed CS preparations triggered contact activation. All implants demonstrated excellent biocompatibility, with implants of Group A and B showing excellent features as osteoconductive and -inductive scaffolds able to improve mechanical stability.

Graphical abstract

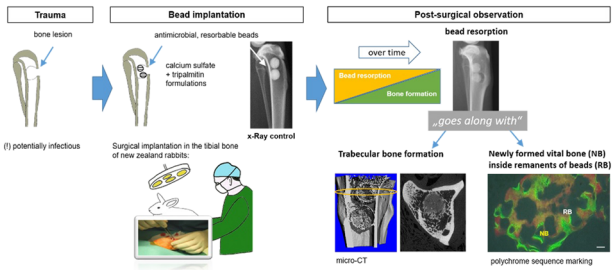

R. Burgkart and A. Obermeier contributed equally to this work.

D. Pförringer and N. Harrasser contributed equally to this work.

✉ D. Pförringer
Dominik.Pfoerringer@mri.tum.de

[1] Klinikum rechts der Isar der Technischen Universität München, Klinik und Poliklinik für Unfallchirurgie, München, Germany

[2] Klinikum rechts der Isar der Technischen Universität München, Klinik für Orthopädie und Sportorthopädie, München, Germany

[3] Chirurgisches Klinikum München Süd, München, Germany

1 Introduction

Bone defects as a result of major trauma, infection or bone tumor represent a challenge for reconstructive surgery. Depending on the defect's extent, bone grafting is used as an established method. In addition bone grafts can be antibiotically loaded to prevent or treat infections [1]. The missing bone is replaced with material from the patient's own body (autologous), artificial, synthetic, or natural (heterologous) substitutes. The final fate of a bone graft is highly dependent on local phenomena such as osteoconduction, osteoinduction, and osteogenesis [2]. Autologous grafts are considered as gold standard for defect reconstruction. However, their use is not without restrictions as donor site morbidity and limited availability pose common concerns. An alternative approach for defect reconstruction can be through the use of allografts. Again, limitations commonly associated are the potential for disease transmission, immunogenic response, and quality variability. Therefore, research activities have been focused on attempts to create ideal artificial bone grafts. Calcium sulfate (CS) is an inexpensive material known for its high biocompatibility [3]. Furthermore, CS allows the incorporation of therapeutic substances and can function as a carrier material for drugs, which extends its usability in the field of bone reconstruction [4, 5]. Additionally, CS acts primarily as an osteoconductive structure for ingrowing bone, for newly formed host bone to replace the material simultaneously without inducing a significant inflammatory reaction [6]. CS lacks intrinsic osteoinductive or osteogenic capacity, and CS resorption usually occurs faster than bone formation [7]. A possible way to antagonize this is the addition of osteoinductive and/or osteogenic components. In this context, hydroxyapatite (HA) has shown favorable results [8, 9]. However, the main limitation for the use of HA ceramics is the inherent brittleness and difficulty in processing [10]. Another promising additive is calcium carbonate. It has been shown that resorption of the CS can leave porosities enhancing the ingrowth of bone. In the present study, we analyzed the biological remodeling in response to implantation of new formulations of CS augmented with antibiotics and calcium carbonate/tripalmitin in rabbit tibiae. Bone ingrowth and biomaterial performance were evaluated using optical microscopy, fluorescence microscopy, conventional radiography and micro-computed tomography (micro-CT) as described in previous literature [11]. Specifically the effect of calcium carbonate/tripalmitin formulations of CS on resorption period was examined. Hence, the provision of temporary structural support during the remodeling process, and thus synchronization of the ingrowing bone with biomaterial resorption, as well as preservation of the bone graft's initial volume were investigated. New formulations for delayed resorption and osteoconduction of artificial bone substitute materials may facilitate the bone regeneration process in an antimicrobial environment. Herewith, trauma and orthopedic surgeons may find a future bone substitute material for complex bone regeneration as infect-prophylaxis, especially in case of methicillin-resistant staphylococcus aureus (MRSA) infections.

2 Material and methods

2.1 Implants

The resorbable bone substitute materials based on CS formulations used in the present study consisted of CS dihydrate, gentamicin, and tripalmitin (Group A: Herafill®-G), CS dihydrate, vancomycin, and tripalmitin (Group B: CaSO4-V), as well as commercially available tobramycin-loaded CS hemihydrate (Group C: Osteoset®) as depicted in Fig. 1. The single beads varied in size and consequently in numbers implanted to match overall implanted mass of approximately 500 mg. For this purpose, two units of Group A implants (500 mg), 14 units of Group B implants (490 mg), and five units of Group C (537.5 mg) were used to implant inside an artificial rabbit tibial bone defect for investigation.

Group A implant at 6.0 mm diameter and 250 mg weight per unit, consists of calcium sulfate dihydrate (71.6%), calcium carbonate (17.9%), tripalmitin (8.8%) and gentamicin sulfate (1.7%). Group B implant at 3.0 mm diameter and 35 mg per unit, consists of calcium sulfate dihydrate (72.0%), calcium carbonate (18.0%), tripalmitin (8.9%) and vancomycin hydrochloride (1.1%). Group C implant at 4.8 mm diameter and 107.5 mg weight per unit, consist of a hemihydrate modification of calcium sulfate (96.0%) and tobramycin sulfate (4.0%). Composition of bead implants is given in contents per weight.

2.2 Animal study—protocol

The study was approved by the Animal Experimentation Ethics Committee of Bavaria (Reg. No. 209.1/211-2531.2-22/05) and conducted with reference to the OECD Principles of Good Laboratory Practice. 54 female New Zealand white rabbits (Charles River Laboratories, Sulzfeld, Germany) with a mean body weight (BW) of 4.5 kg (range: 4.3–4.7 kg) underwent surgery. For acclimatization purposes, the animals were delivered to the facility atleast two weeks prior to surgical intervention. Animals were housed in cages (2–3 animals) at normal room temperature and daylight illumination with ad libitum access to food and water. The animals were divided in 3 groups according to the test implant groups (Table 1).

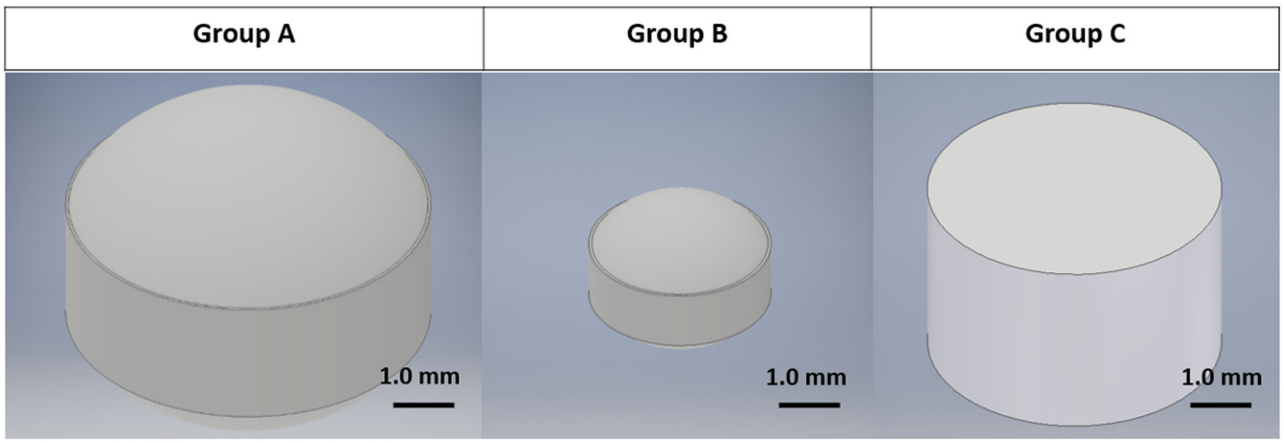

Fig. 1 Bead implants used for this study based on calcium sulfates containing antibiotics. Bead implants used for the in vivo animal study: gentamicin-containing Herafill®-G (Heraeus Medical, Inc., Germany) beads (Group A), CaSO4-V using vancomycin beads (Group B), and tobramycin incorporated Osteoset® implants (Group C)

Table 1 Study protocol according to number of animals and day of sacrifice

	Group A (Herafill®-G)	Group B (CaSO4-V)	Group C (Osteoset®)
Animals per group	18	18	18
Number of animals/week of sacrifice	4/4	4/4	4/4
	4/6	4/6	4/6
	5/8	5/8	5/8
	5/12	5/12	5/12

Groups of animals used for the in vivo pre-clinical rabbit study. Each Group (A–C) using a different type of bone substitute material contains 18 rabbits, sacrificed after 4, 6, 8, and 12 weeks after implantation respectively

2.3 Animal study—surgical procedure

Surgery was performed under general anesthesia utilizing weight-adapted intramuscular injection of Medetomidine 0.25 mg/kg BW (Domitor®, Pfizer Inc., Germany) and Ketamine 17 mg/kg BW (S-Ketanest®, Parke-Davis GmbH). Analgesia during surgery was obtained through intravenous application of Metamizole 30 mg/kg BW (Novaminsulfon®, Ratiopharm GmbH, Germany) at the beginning of surgery. The left hind leg undergoing surgery was shaved, and the skin cleaned antiseptically (Cutasept®, Bode Chemie, Germany). The skin incision was placed laterally of the tibial tuberosity, consequently bone manipulation was performed at the medial side. This local skin displacement was utilized to prevent infection of the implant site through the skin wound. A water cooled surgical diamond fraise was employed to drill an 8 mm spherical bone cylinder to open the medullary cavity. Using a sterile forcep beads were inserted into the proximal medullary cavity. Differing number of implants had to be inserted according to varying size of beads to match overall implanted mass of 500 mg (±8%) (Group A: 2 units, Group B: 14 units, and Group C: 5 units). After implantation, the cavity was closed using the initially removed bone cylinder while surgical site was irrigated using sterile saline. Subcutaneous tissues were readapted (3–0 Vicryl®, Ethicon GmbH, Germany), and skin closed (3–0 Prolene®, Ethicon GmbH, Germany). Thereafter, a spray bandage (Opsite®, Smith & Nephew PLC, England) was applied. Anesthesia was antagonized using Atipamezole 0.25 mg/kg (Antisedan®, Pfizer Inc., Germany).

Buprenorphine (0.03 mg/kg BW s.c., Temgesic®, Essex Pharma GmbH, Germany) was administered for analgesia towards the end of the surgical procedure immediately before wound closure was completed and postoperatively every 8 h for 4 days. In addition, Carprofen 4 mg/kg s.c. (Rimadyl®, Pfizer Inc., Germany) was given for 7 days every 12 h. Animals underwent daily control examinations considering general condition, body temperature and surgical site of the operated leg. Blood was obtained (from an ear vein) at the end of the surgical procedure and weekly until sacrifice of the animal to determine blood count, and calcium/alkaline phosphatase levels.

Animals were euthanized after 4, 6, 8, and 12 weeks according to different testing groups (Table 1) employing an overdose of Pentobarbital-sodium (Narcoren®, Merial GmbH, Germany 50 mg/kg). The tibiae were dissected. Then, all soft tissue was stripped from the bone, which was consecutively stored in 100% methanol.

2.4 Radiography

Immediately after surgery and at the end of each observation period, the tibiae were X-rayed via contact-radiography in a lateral view using an X-ray generator at 44 kV and 4

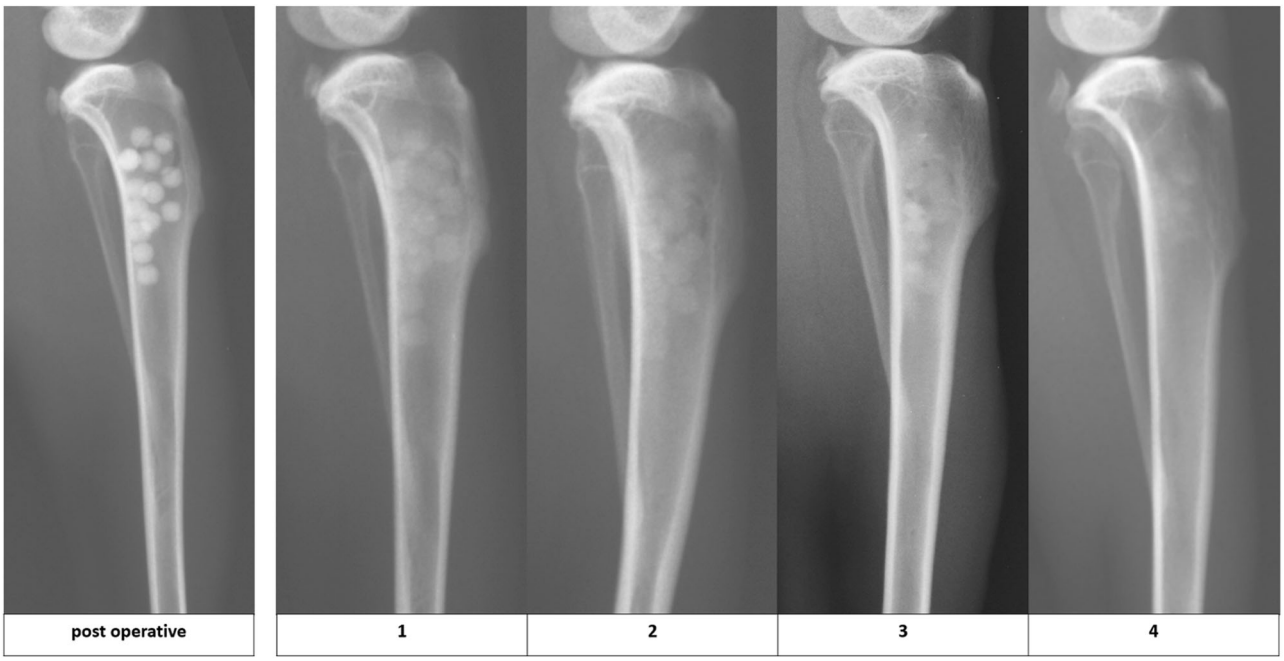

Fig. 2 Scoring system for radiographic changes. Scoring system for x-ray pictures to evaluate the grade of resorption (1: radiopaque locally reduced; 2: radiopaque uniformly reduced; 3: implants shadowy; 4: implants completely disbanded)

mAs (Super 80CP, Philips GmbH, Germany). Evaluation of radiographic changes was performed semi-quantitatively (Fig. 2).

2.5 Micro-CT

Additionally, micro-computed tomography (micro-CT 80, Fa. Scanco, Brüttisellen, Switzerland) of the explanted tibiae was carried out (Fig. 3). Images were obtained as transverse planes of the tibia and were further processed as 3-dimensional reconstructions to get an overview. All micro-CTs were performed on dissected tibiae after sacrifice of the animals.

2.6 Histology

Histomorphological analysis was performed to evaluate bone growth and bone vitality around the implants using two kinds of staining. In vivo fluorochrome substances were injected postoperatively at fixed time intervals to achieve a fluorescent labeling of newly formatted bone. Additionally, a classical histomorphological staining of specimen surfaces was performed after polymerization and down polishing of tibiae ex vivo.

Histological specimens were prepared via embedding with methyl-methacrylate resin (Technovit® 4004, Heraeus Kulzer GmbH, Germany) and dissecting mid-tibiae sagittally utilizing a diamond saw (Exakt 300CL, Exakt GmbH, Germany), followed by grinding down with a polishing machine (Planopol-V and Pedemax-2, Struers GmbH, Germany) to a thickness of 40–120 µm with diamond discs to get histological slides.

Approximately 100 µm thick tibia sections of every group at 4, 6, 8, and 12 weeks were then histomorphologically stained with a modified Grünwald-Giemsa-staining called "K2". This staining is suitable to evaluate the newly formed bone, with newly formed osteoid tissue stained yellowish-brown, old bone stained light-green/blue, connective tissue stained orange-red and calcifications stained bright-greenish-blue. The surface stained specimens were then investigated via photo macroscopy (Wild M400, Wild Heerbrugg AG, Switzerland) at 2× magnification to get an overview and using light microscopy (DMRB, Leica Microsystems GmbH, Germany) for more detail at 25× and up to 250× magnifications.

All implants and surrounding tissue were evaluated for osteogenesis (criteria: amount of trabecular bone formation, number of osteoblasts, amount of osteoid, general impression) and amount of implant resorption (criteria: lysis of implant surface, presence and number of surrounding giant cells, general inspection of morphology). Osteogenesis was graded on a scale from 1 to 3 (little to maximum), resorption of implants from 1 to 4 (none to complete) (Fig. 4).

To measure bone apposition rates after surgery (i.e., the rate of bone ingrowth or bone deposition) within and around the implants, five separate fluorochrome labels were

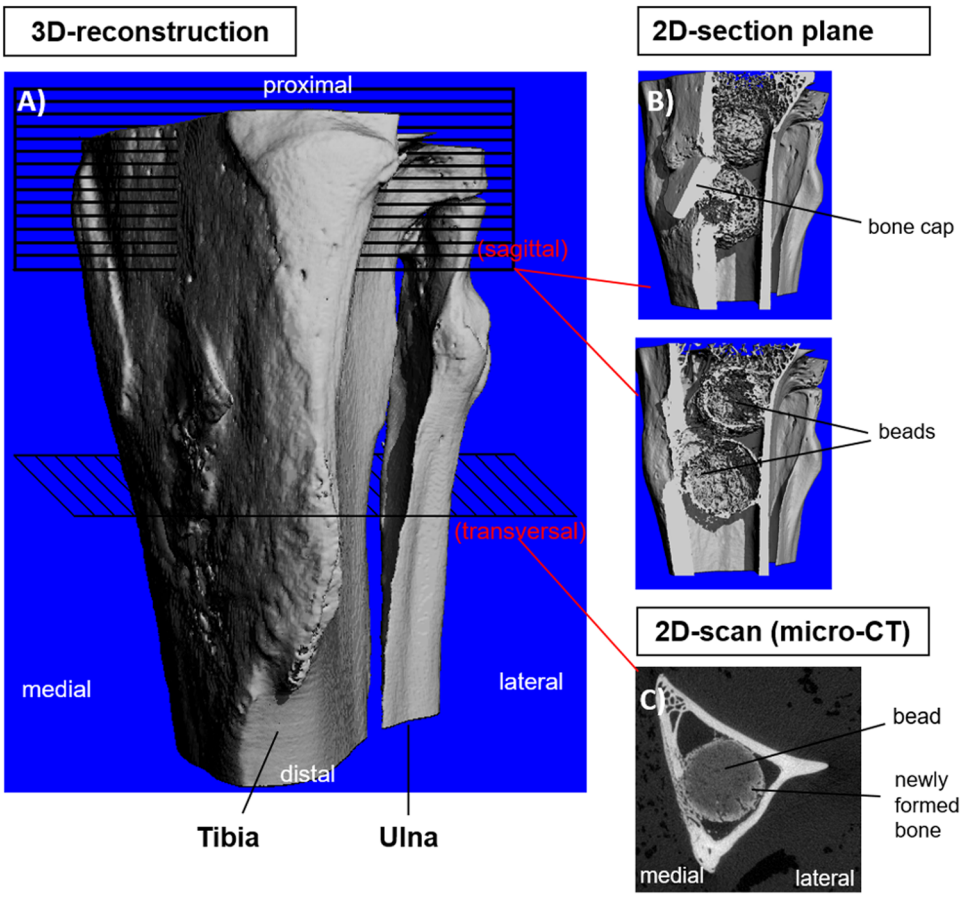

Fig. 3 Explanation of micro-CT planes used for tibia of a sacrificed animal (Group A, after 6 weeks). Exemplary declaration of micro-CT planes used in sacrificed rabbits from group A after 6 weeks: **a** 3D-reconstruction was carried out for gross overview; 2D-section plane in the sagittal direction **b** and the transversal plane from micro-CT scan **c** were analyzed for bone ingrowth and implant degradation

administered subcutaneously. For this purpose different fluorochrome solutions were injected at the following days postoperatively: 21 and 22 days (tetracycline, 30 mg/kg BW), 35 and 36 days (alizarine-complexon, 30 mg/kg BW), 49 and 50 days (calcein green, 30 mg/kg BW), 63 and 64 days (xylenol orange, 90 mg/kg BW), and 77 and 78 days (calcein blue, 30 mg/kg BW). Fluorochrome labels are bound to sites of active bone deposition shortly after administration [12]. Therefore, the time of bone formation can be related to the individual fluorescence color of each fluorochrome label administered chronologically.

Later on, specimens were investigated with their fluorochrome labeling, because of new bone formation using a light microscope (DMRB, Leica Microsystems GmbH, Germany) with an ultraviolet light source and at 25x and up to 250x magnifications. Polychrome sequence marking was performed during the time of postoperative observation, exemplarily for one animal of each group. The fluorescence evaluation was performed at weeks 8 and 12.

Fluorescence colors of bone tissue specimens indicate the time of bone formation, correlating with the time of fluorescence stain application in vivo. Thus, time of bone formation can be assigned to individual label colors (Table 2).

2.7 Statistical analysis

Experimental investigations via x-ray, micro-CT and classical histology were conducted by atleast 4-fold replicates. Therefore, the smallest group of animals used to sacrifice on each time point at 4, 6, 8, and 12 weeks post-surgical were 4 animals. One animal for each group was sacrificed additionally at weeks 8 and 12, in order to achieve specimens for fluorescence microscopy after polychrome sequence labeling. Scores for x-rays and classical histological (modified Giemsa stain) pictures were generated to collect semi-quantitative information regarding the grade of implant resorption as well as osteogenesis. Due to the semi-quantitative dataset statistical calculation of significant levels was not performed.

3 Results

3.1 Animal surgery and post-surgical period

All rabbits tolerated the surgery and passed the follow-up period without complications. The animals were fully weight-bearing on the first post-operative day. All implants

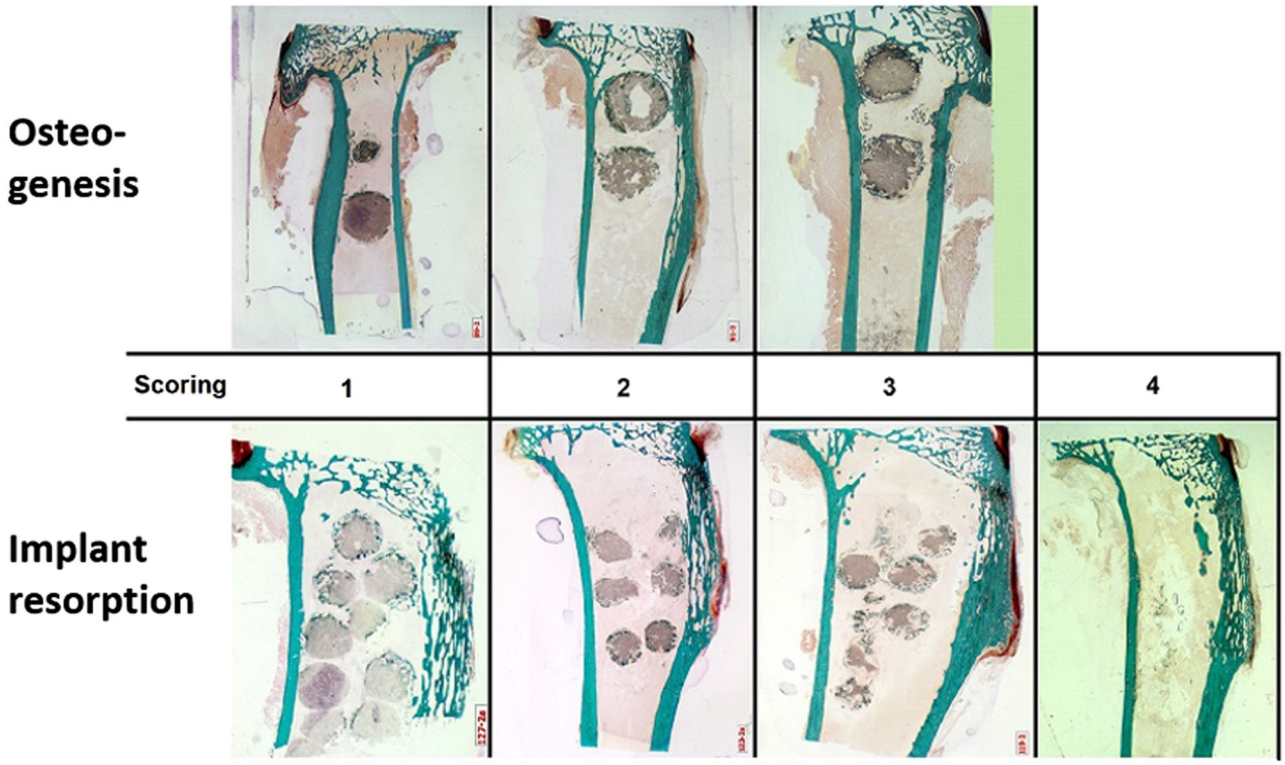

Fig. 4 Histological scoring system (modified Giemsa-stain) for osteogenesis (group A) and implant resorption (group B). Histological scoring system (modified Giemsa-stain) for osteogenesis (1: no osteogenesis, 2: $<50\%$ of implant circumference with signs of osteogenesis, 3: $>50\%$ of implant circumference with signs of osteogenesis) and implant resorption (1: $<10\%$ of implant degraded, 2: 10–50% of implant degraded, 3: $>50\%$ of implant degraded, 4: $<10\%$ of implant remnants detectable)

Table 2 Correlation of fluorescence color and bone formation time

Substance	Time of bone formation (post-operative week)	Fluorescence color (UV excitation)
Tetracycline	3	Yellow/green
Alizarine-complexon	5	Red
Calcein green	7	Green
Xylenol orange	11	Orange

Correlation of fluorescence color of newly formed bone dependent on substance solution and time of administration used. Resulting in visually distinguishable stains of newly formed bone at different time periods by defined colors

were tolerated well. Local signs of infection were not observed.

3.2 Radiography

Conventional radiographs showed differences of biodegradation between the implants over time. Initially, four weeks after implantation, all beads were radiographically detectable at the level of the initial insertion sites. Evaluation of changes in radio-opaqueness (Table 3) revealed no relevant changes from the 4th to the 12th week, with well distinguishable beads at 12 weeks in group A. On the other hand, radiolucency of the beads increased over the study period in groups B and C. In group B radiolucency increased uniformly every 2 weeks starting from the 4th with completely disbanded implants at 12 weeks. In group C the implants were only faintly detectable after the 4th

Table 3 Evaluation of the radiopaqueness of implants

Group		A	B	C
Sacrifice (week)	4	1.0 ± 0.0	1.8 ± 0.3	2.5 ± 1.0
	6	2.0 ± 0.0	2.3 ± 0.3	4.0 ± 0.0
	8	1.8 ± 0.2	3.0 ± 0.0	4.0 ± 0.0
	12	2.0 ± 0.0	3.8 ± 0.2	4.0 ± 0.0

Evaluation of radiopaque implants from 4 to 12 weeks of the single groups. All data is given as mean $\pm$ standard deviation (1: representing the minimum and 4: the maximum degree of resorption)

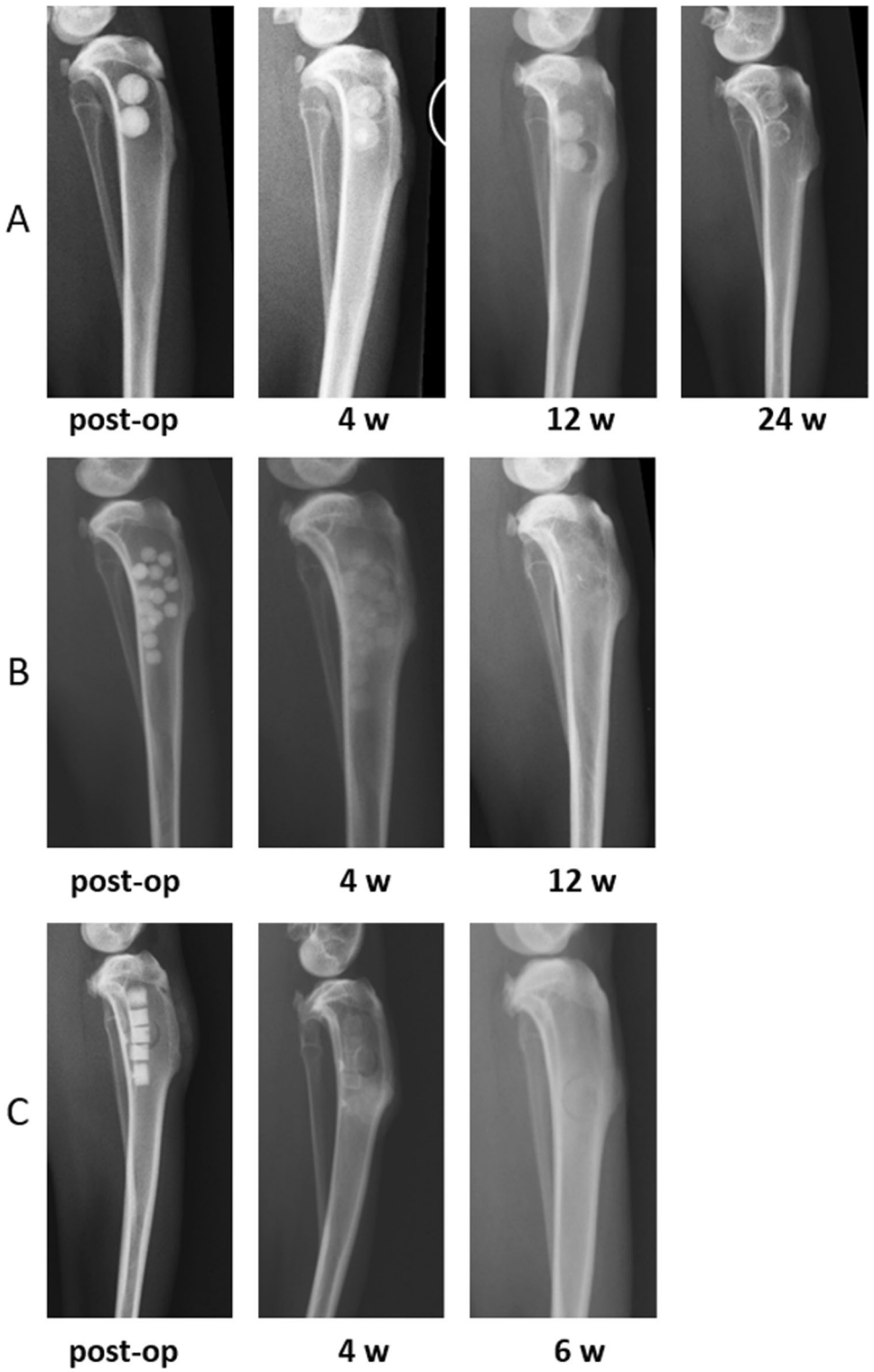

Fig. 5 Time of implant resorption over time via x-ray opaqueness. Evaluated time intervals of implant resorption for each group of implants used. **a** Herafill®-G, **b** CaSO4-V, and **c** Osteoset® during implantation via x-ray opaqueness

week and had already disappeared radiologically after 6 weeks.

The relevant time points for evaluation of the implant resorption time is given in Fig. 5, exemplarily for each group. Especially for group A, a prolonged observation time of 24 weeks was used.

3.3 Micro-CT

In group A all investigated implants showed radiopaque cores and localized mineralized surface changes after 4 weeks. Two of four animals showed beads with well distinguishable trabecular structures between the

implant's surface and the host bone cortex. After 6 weeks the radiopaque core of all implants had disappeared, and the surface was homogenously disorganized due to resorption. Additionally, cortical bone bridges reached all implants. After 8 and 12 weeks, bone bridging on the implants had progressed, while resorption of the implants had not changed.

Almost complete resorption for group B and C was detected within 12 and 6 weeks, respectively. The implants were almost completely resorbed in all animals. Varying degrees of mineralization at the periphery of the implant bed were detected. Group B indicated a delayed resorption until the 12th week and superficial trabecular structures, compared to pure calcium sulfate containing Group C implants. Bone bridges from the animals' cortex to the mineralized areas were found in a smaller quantity in group B, but not for Group C implants.

An overview of the micro-CT evaluations over the time of observation is given in Fig. 6, using the data of one representative animal for each group. In general, this data confirms the post-surgical course of radio-opacity, related to the time of resorption, for each type of implant in vivo.

3.4 Histology

In group A, after 4 weeks trabecular bone formation, invasion of osteoblasts and erosion was detectable on all implants' surfaces. These mechanisms protruded up to 12 weeks with still detectable implants and surrounding giant cells at the time of sacrifice.

In group B, changes already described for group A were also visible after 4 weeks. Implant resorption was more pronounced compared to group A with almost fully degraded implants after 12 weeks. Giant cells were not detectable from week 8 onwards.

In group C, osteogenesis was comparable to the findings of group B with invasion of osteoblasts and production of osteoid starting from week 4. Resorption was very pronounced with almost fully resorbed implants from week 6 onwards. There were no more recognizable beads after 12 weeks. All histological data is given in Table 4.

The following Fig. 7 shows the results of histological evaluation over time as an overview, exemplarily depicted on one specimen.

These histological slices confirm the findings from x-Ray and micro-CT results. Especially, the osteogenesis vs. implant resorption can be seen along the time axis.

Figure 8 depicts the results of histological evaluation over time in more detail using histological staining for bone mineralization.

Analysis of the histological specimen by means of polychrome sequence marking after 8 and 12 weeks revealed the periimplant bone as newly formed vital bone with the enhancement of applied fluorochromes (Fig. 9).

In the newly formed bone, no evidence of foreign body response to the biomaterials (e.g., presence of inflammatory cells or fibrous tissue) was observed.

4 Discussion

Rapid and complete reconstruction of bone defects through autologous or allogeneic bone or bone-related tissue is crucial in trauma and orthopedic surgery. Calcium sulfate (CS), also known as plaster of Paris, has been used for multiple implications for more than a century [13]. For several years, its use in the surgical setting has been proposed [2]. Key features of this bone graft substitute include its biocompatibility, and its use as a binding and stabilizing agent. Additionally, the matrix is osteoconductive, which leads to new osseous in-growth [14, 15]. On the other hand, rapid resorption rate limits its use as a structural allograft. In this context, some authors found unsatisfactory results for CS if used as a bone graft [16]. We had anticipated that a combination of CS with calcium carbonate/tripalmitin, can purposely delay the degradation process, providing temporary structural support during the remodeling, synchronizing the ingrowing bone with biomaterial resorption, and preserving the bone graft's initial volume. The present study aimed to visualize the mechanisms of bone formation in the presence of novel antibiotic impregnated CS implants in a rabbit model. With the use of radiographic and histologic methods, none of the three tested bead formulations (Herafill®-G (A), CaSO4-V (B), and Osteoset® (C)) displayed any adverse reactions, while all of them were undergoing atleast partial decomposition within the tibial bone.

These three bone substitutes composed of CS, differing side groups consisting of dihydrate (A and B) and hemihydrate (C) in combination with differing antibiotics (gentamicin (A), vancomycin (B), and tobramycin (C)) were used as study implants. Beads of group C, consisted of a hemihydrate formulation of CS and are commercially available (Osteoset®). In contrast, beads of group A and B are novel preparations consisting of CS dihydrates with calcium carbonate and tripalmitin. Also, Group A (Herafill®-G) is a commercial product, whereas Group B is still in the development stage to treat MRSA infections in the future. The rationale for the use of calcium carbonate as an additive is its ability to delay degradation of CS and buffer the pH value in the implant region thus counteracting healing problems of the tissue [17, 18]. Tripalmitin as a fatty acid influences the release kinetics of the antibiotics gentamicin and vancomycin to allow the beads to act potentially antimicrobially over a longer period of time [19, 20].

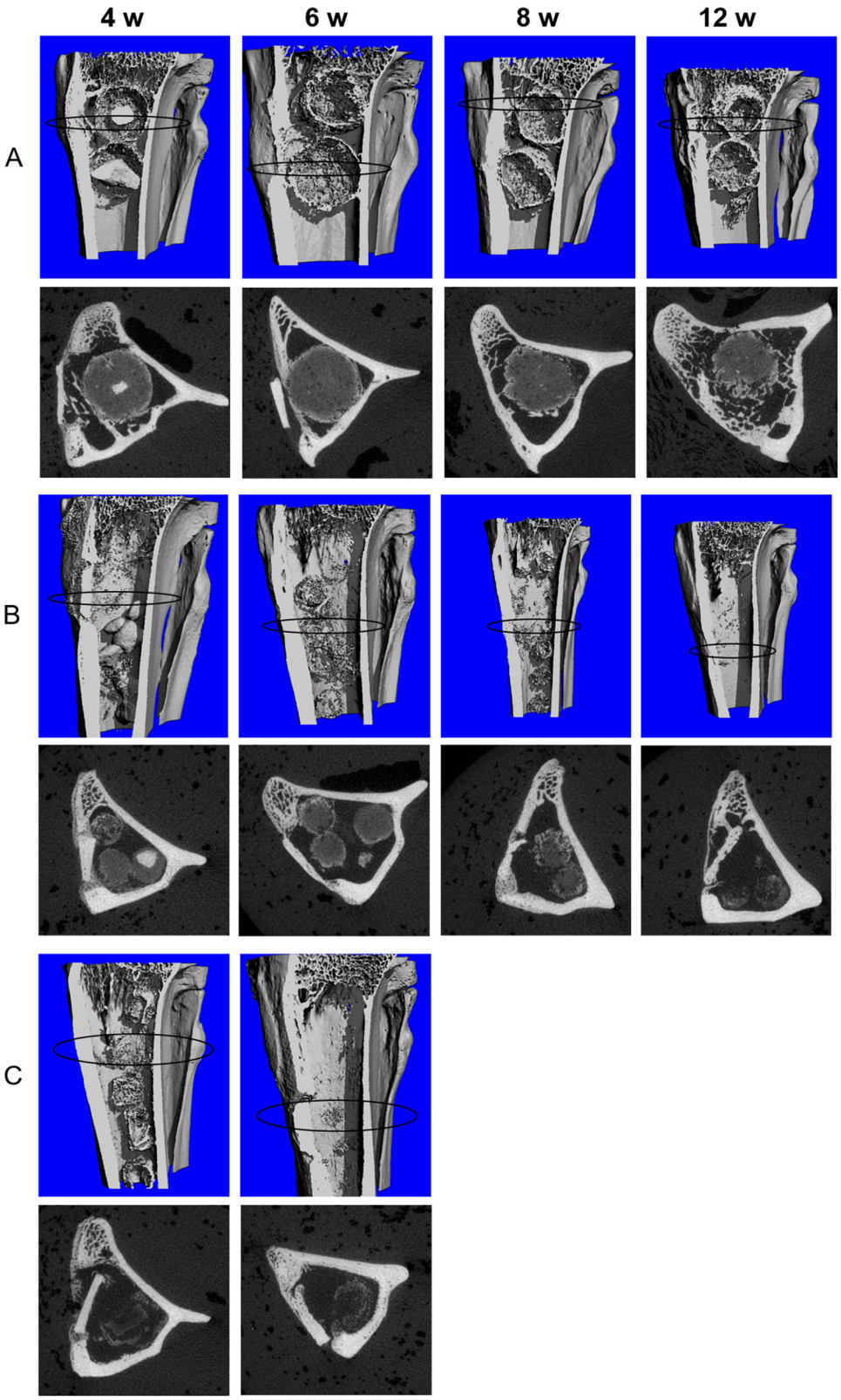

Fig. 6 Resorption and trabecular bone formation over time via micro-CT. Overview of the micro-CT evaluation for each implant group **a** (Herafill®-G), **b** (CaSO4-V), and **c** (Osteoset®) over the time of observation 4, 6, 8, and 12 weeks. The first row of each group shows a virtually opened 3D-model, reconstructed from micro-CT. Second rows show 2D micro-CT cross-section pictures, position of planes marked in the 3D-model with a black ellipse

The tibiae were analyzed by different methods, in which drug release kinetics had already been described [13]. Conventional radiographs allowed a statement on the rate of resorption of implants during the study period. Further examination by micro-CT enabled a more precise insight into the processes of bone formation and implant resorption.

While the 3-D reconstructions gave an overview of the processes in the interior of the entire bone, the main disadvantage is the influence on the image by adjusting black and white values. On the other hand, the transversal 2-D images reflect the unaltered facts and ongoing visible mechanisms at the bone–implant interface. However, the amount of pictures is not suitable for an overview. Therefore, the combination of both views is essential for analysis of the mechanisms acting around the implants.

Table 4 Evaluation of osteogenesis/implant resorption

Group			A (Herafill®-G)	B (CaSO4-V)	C (Osteoset®)
Osteogenesis	Sacrifice (week)	4	2.0 ± 0.5	1.8 ± 0.3	2.2 ± 0.3
		6	2.0 ± 0.9	1.5 ± 1.0	1.3 ± 1.0
		8	2.0 ± 1.0	1.5 ± 0.5	1.5 ± 0.0
		12	2.0 ± 0.5	0.8 ± 0.3	1.7 ± 0.3
Implant resorption	Sacrifice (week)	4	2.2 ± 0.3	2.2 ± 0.3	2.8 ± 0.3
		6	2.3 ± 0.3	2.2 ± 0.8	3.5 ± 0.9
		8	2.5 ± 0.5	2.3 ± 0.6	3.7 ± 0.3
		12	2.3 ± 0.6	3.7 ± 0.3	4.0 ± 0.0

Evaluation of osteogenesis/implant resorption from 4 to 12 weeks of the single groups. All data is given as mean ± standard deviation. (1: representing minimum degree of resorption, 4: representing maximum degree of resorption)

Resorption of the beads between the groups of this study differed considerably (Table 4). The implants of group C consisted only of CS and tobramycin and had already shown peripheral and central signs of resorption in the 4th week. In the 6th and especially the 8th week after implantation, beads had almost fully degraded. Beads of group B were no longer detectable radiologically after the 12th week, while the micro-CT scans and histological slices showed remnants of the beads as well as low amounts of bone formation around the former implant sites. This observation was supported by the data of the polychrome sequence marking. The beads of group A (Herafill®-G)

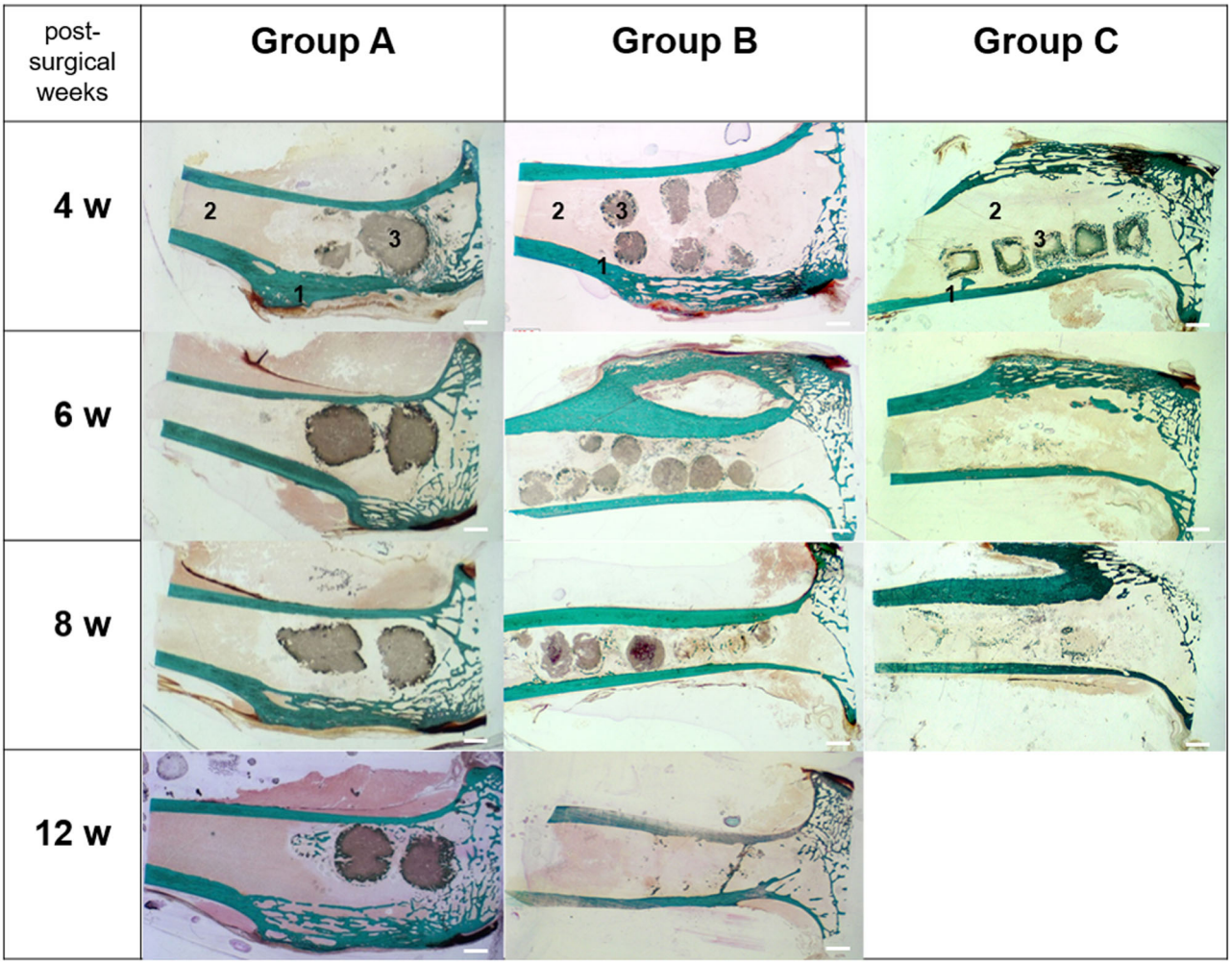

Fig. 7 Histological slices of each group: time overview. Histological slices using an overview perspective (magnification 2x) to show the implant degradation over time for each group. **a** Herafill®-G and **b** CaSO4-V over 12 weeks, as well as **c** Osteoset® over 8 weeks (1: cortical bone; 2: medullary cavity; 3: bead implant). The white scale bars indicate 2 mm length

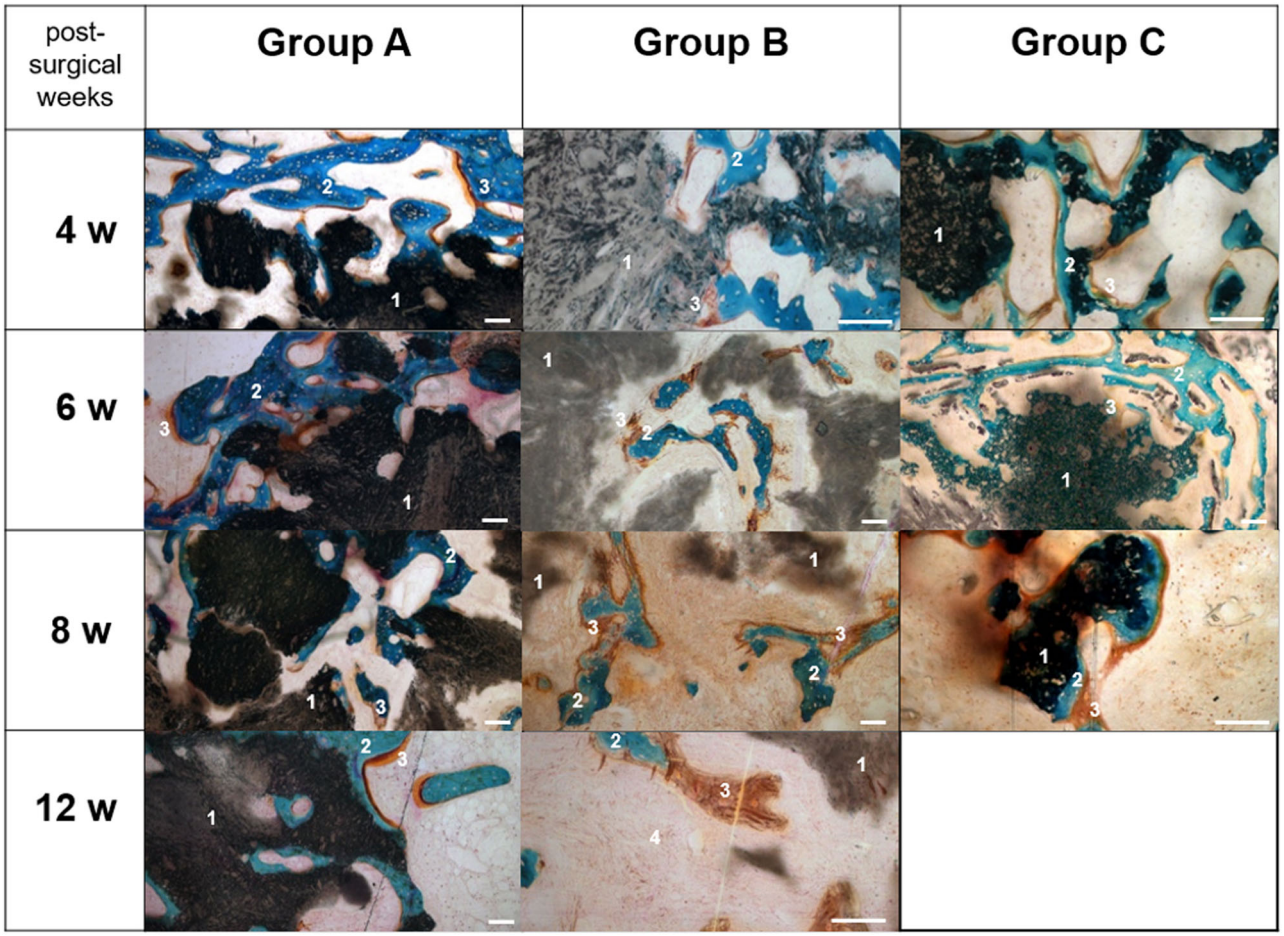

Fig. 8 Histological slices of each group over time in more detail. Histological slices more in detail over time to show the mineralized bone and osteoid formation in the ongoing of implant degradation for each group. **a** Herafill®-G, **b** CaSO4-V and **c** Osteoset® (1: bead implant; 2: mineralized bone; 3: osteoblasts at osteoid synthesize; 4: phagocytes). The white scale bars represent 100 µm length

were well detectable radiographically after 4 weeks. In the 6th week increasing radiolucency of the beads was detectable, which increased up to week 8. At week 12 no further changes were shown. These observations suggest that both the size and composition of the implants influence the degradation rate. For Osteoset®, CS alone (group C), a faster degradation was observed than for the compositions containing tripalmitin and calcium carbonate (group A and B (CaSO4-V)). Within the latter group, the size of the implants seems to play an important role, since the small beads of group B were absorbed more rapidly than the large beads of group A. These findings are in accordance to reported data from literature, where different degradation times for CS are reported for different sizes of implants: 3–4 weeks [21], 4–10 weeks [22], 6 weeks [23], 5–7 weeks [24], 45–72 days [3, 25], 8 weeks [26], 2–4 months [17] and 6 months [27]. This shows that size correlates directly with resorption time. Additionally, the localization of implantation influences degradation time as presented on beads in the radius [3], tibia [28], femur [28] or maxilla and mandible [29, 30]. Lastly, the used animal model can also influence the degradation as already investigated in the dog [3, 29, 30] or rabbit [21].

By means of histological staining in the present study, we were able to find deep lacunae in the periimplant bone of all three formulations as clear signs of cellular degradation. Additionally, the presence of multinucleated giant cells on or in the implant material confirms the presence of cellular degradation. Regarding the nature of CS degradation contradicting mechanisms have been described. Bell et al. and Tay et al. argue that CS degrades through the process of dissolution [24, 26]. This supports other investigators, who explain accelerated bone formation by provision of calcium ions during the degradation process [21]. Walsh et al. conclude that the pH reduction leads to a demineralization of the adjacent bone, which subsequently leads to a release of BMP, which in turn stimulates bone regeneration [31]. Sidqui et al. also noted in their study that the activity of osteoclasts was excited by an acidic pH [32]. Other authors however argue that CS is degraded by cellular phagocytosis

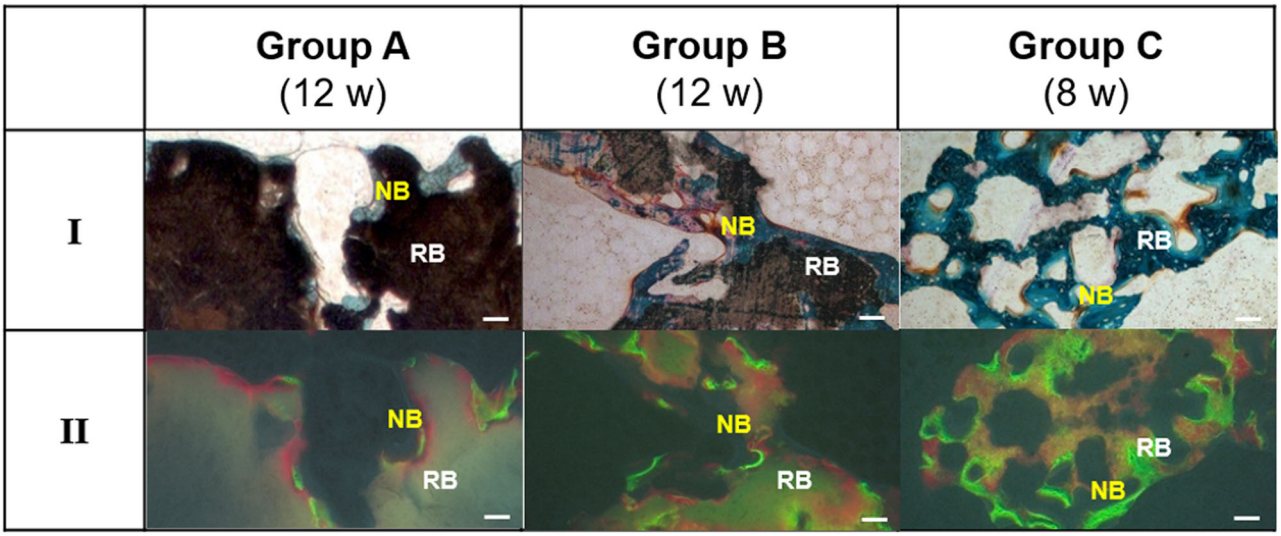

Fig. 9 Histological slices and fluorochrome labeled bone at the implants in tibia of each group. Histological slices (I) and fluorochrome labeled bone (II) of tibia of each group A–C after 12 weeks (**a** Herafill®-G and **b** CaSO4-V), as well as after 8 weeks (**c** Osteoset®). Corresponding to histological pictures fluorochromes were deposited around and inside the beads (NB new bone; RB remnants of beads). (II) Fluorescence colors indicate newly formed bone at different post-surgical periods (yellow/green (3w): tetracycline; red (5w): alizarine-complexon; green (7w): calcein green; orange (11w): xylenol orange). The white scale bars represent 100 µm length

[3]. Orsini et al. report in their study of a combination of both dissolution and cell-mediated degradation of CS [33]. However, whether CS additionally is degraded by dissolution cannot be stated with the findings of the present study.

The osteoconductive potential of CS was clearly detected in this study. All three formulations showed invading osteoblasts with active production of osteoid at the implant sites and walled osteocytes with surrounding newly formed bone at the level of the implants' surfaces and in the resorption lacunae. Group C showed osteogenesis up to the 8th week, with only remnants of osteoid at the level of the former implant site up to the 12th week (Table 4). Similar events were found in group B, with active osteogenesis from the 4th week starting and decreasing over time. Group A beads seemed to induce osteogenesis at a steady-state level from the 4th up to the 12th week. Here, fine cortical bone trabeculae bridged the implant-bone interface at day of sacrifice. Possibly, the osteoconductive effect of group B may be improved to the level of group A by using larger bead dimensions. In summary, osteogenesis was found to decrease over time in group B and C almost parallel to degradation of the beads. On the other hand, high levels of osteogenesis in group A were detected over 12 weeks. These mechanisms were also supported by polychrome sequence marking after 12 weeks. In all three formulations, clear osteogenic signs detecting bone formation in direct contact to the degrading implants were found.

One limitation of this study is the use of different sizes for implants employed. The weights of the beads in sum were comparable by accordingly using different numbers of beads per type. To allow for an ideally comparable situation, beads of exact same size and antibiotic content should be used. However, this study delivers valid results for resorption and bone formation over time, as the use of real market ready material was compared. Molecular biologic methods in future studies might help in further evaluation of the newly formed bone inside and around the implants during resorption.

In summary, the present study supported the biocompatibility of novel antibiotic impregnated CS beads and specified the mechanisms in a rabbit model. The addition of calcium carbonate/tripalmitate delayed the degradation of the implants and resulted in synchronization of the ingrowing bone with biomaterial resorption but did not have negative effects on biocompatibility. Further in vivo studies are needed, in order to estimate time for complete resorption of these new formulations of CS beads and to determine responses of bone cells to this biomaterial.

5 Conclusion

In a rabbit model novel formulations of absorbable bone substitute materials based on calcium sulfate exhibit delayed time of resorption, while osteoconduction is facilitated. Moreover, a sustaining osteogenic effect is determined over 12 weeks after implantation for Herafill®-G beads. The use of novel calcium sulfate based bone substitute materials, incorporated with calcium carbonate/tripalmitin and antibiotics can stimulate the bone regeneration process in an antimicrobial environment. Herewith, trauma and orthopedic surgeons may receive a future bone

substitute material for complex bone regeneration as well as infect-prophylaxis.

Acknowledgements At first, we would like to thank Mr. Dr. H. Büchner and Mr. Dr. S. Vogt (Heraeus Medical GmbH, Werheim, Germany) for their kind supply of bone substitute materials (Herafill®-G, as well as CaSO4-V). Second, many thanks to the central preclinical research division (ZPF) of the Klinikum rechts der Isar at the Technical University of Munich for their excellent support in performing the animal study. Especially, many thanks to Mrs. Dr. M. Rößner and Prof. Dr. H. Gollwitzer for their guidance in surgical procedure. Also, many thanks to Mrs. Dr. S. Kerschbaumer for generating and interpreting histological slices. Moreover, special thanks to Prof. Dr. P. Augat (Department of Biomechanics at the Unfallklinik Murnau) for his kind support in micro-CT investigations. Finally, many thanks to Mr. F. Seidl (M.A. Interpreting and Translating, MBA) for his kind support due to his perfect command of scientific English.

Compliance with ethical standards

Conflict of interest The authors declare that they have no conflict of interest

References

1. Lalidou F, Kolios G, Drosos GI. Bone infections and bone graft substitutes for local antibiotic therapy. Surg Technol Int. 2014;24:353–62.
2. Cortez PP, Silva MA, Santos M, et al. A glass-reinforced hydroxyapatite and surgical-grade calcium sulfate for bone regeneration: In vivo biological behavior in a sheep model. J Biomater Appl. 2012;27:201–17. https://doi.org/10.1177/0885328211399479
3. Peltier LF. The use of plaster of paris to fill large defects in bone. Am J Surg. 1959;97:311–5.
4. Helgeson MD, Potter BK, Tucker CJ, Frisch HM, Shawen SB. Antibiotic-impregnated calcium sulfate use in combat-related open fractures. Orthopedics. 2009;32:323.
5. Beuerlein MJ, McKee MD. Calcium sulfates: what is the evidence? J Orthop Trauma. 2010;24(Suppl 1):S46–51. https://doi.org/10.1097/BOT.0b013e3181cec48e
6. Thomas MV, Puleo DA. Calcium sulfate: Properties and clinical applications. J Biomed Mater Res B Appl Biomater. 2009;88:597–610. https://doi.org/10.1002/jbm.b.31269
7. Slater N, Dasmah A, Sennerby L, Hallman M, Piattelli A, Sammons R. Back-scattered electron imaging and elemental microanalysis of retrieved bone tissue following maxillary sinus floor augmentation with calcium sulphate. Clin Oral Implant Res. 2008;19:814–22. https://doi.org/10.1111/j.1600-0501.2008.01550.x
8. Parsons JR, Ricci JL, Alexander H, Bajpai PK. Osteoconductive composite grouts for orthopedic use. Ann N Y Acad Sci. 1988;523:190–207.
9. Stubbs D, Deakin M, Chapman-Sheath P, et al. In vivo evaluation of resorbable bone graft substitutes in a rabbit tibial defect model. Biomaterials. 2004;25:5037–44. https://doi.org/10.1016/j.biomaterials.2004.02.014
10. Fan X, Ren H, Luo X, et al. Mechanics, degradability, bioactivity, in vitro, and in vivo biocompatibility evaluation of poly(amino acid)/hydroxyapatite/calcium sulfate composite for potential load-bearing bone repair. J Biomater Appl. 2016;30:1261–72. https://doi.org/10.1177/0885328215620711
11. Chen X, Zhou XC, Liu S, Wu RF, Aparicio C, Wu JY. In vivo osseointegration of dental implants with an antimicrobial peptide coating. J Mater Sci Mater Med. 2017;28:76 https://doi.org/10.1007/s10856-017-5885-8
12. Frost HM. Tetracycline-based histological analysis of bone remodeling. Calcif Tissue Res. 1969;3:211–37.
13. Pforringer D, Obermeier A, Kiokekli M, et al. Antimicrobial Formulations of Absorbable Bone Substitute Materials as Drug Carriers Based on Calcium Sulfate. Antimicrob Agents Chemother. 2016;60:3897–905. https://doi.org/10.1128/AAC.00080-16
14. J Borrelli, Jr., Prickett WD, Ricci WM. Treatment of nonunions and osseous defects with bone graft and calcium sulfate. Clin Orthop Relat Res. 2003:245–54. https://doi.org/10.1097/01.blo.0000069893.31220.6f
15. Evaniew N, Tan V, Parasu N, et al. Use of a calcium sulfate-calcium phosphate synthetic bone graft composite in the surgical management of primary bone tumors. Orthopedics. 2013;36:e216–22. https://doi.org/10.3928/01477447-20130122-25
16. Glazer PA, Spencer UM, Alkalay RN, Schwardt J. In vivo evaluation of calcium sulfate as a bone graft substitute for lumbar spinal fusion. Spine J. 2001;1:395–401.
17. Coetzee AS. Regeneration of bone in the presence of calcium sulfate. Arch Otolaryngol. 1980;106:405–9.
18. Coraca-Huber D, Hausdorfer J, Fille M, Nogler M, Kuhn KD. Calcium carbonate powder containing gentamicin for mixing with bone grafts. Orthopedics. 2014;37:e669–72. https://doi.org/10.3928/01477447-20140728-50
19. Coraca-Huber DC, Putzer D, Fille M, Hausdorfer J, Nogler M, Kuhn KD. Gentamicin palmitate as a new antibiotic formulation for mixing with bone tissue and local release. Cell Tissue Bank. 2014;15:139–44. https://doi.org/10.1007/s10561-013-9384-y
20. Obermeier A, Matl FD, Schwabe J, et al. Novel fatty acid gentamicin salts as slow-release drug carrier systems for anti-infective protection of vascular biomaterials. J Mater Sci Mater Med. 2012;23:1675–83. https://doi.org/10.1007/s10856-012-4631-5
21. Lebourg L, Biou. C. [The imbedding of plaster of paris in surgical cavities of the maxilla]. Sem Med Prof Med Soc. 1961;37:1195–7.
22. Geldmacher J. [Therapy of enchondroma with a plaster implant--renaissance of a treatment principle]. Handchir Mikrochir Plast Chir. 1986;18:336–8.
23. Petruskevicius J, Nielsen S, Kaalund S, Knudsen PR, Overgaard S. No effect of Osteoset, a bone graft substitute, on bone healing in humans: a prospective randomized double-blind study. Acta Orthop Scand. 2002;73:575–8. https://doi.org/10.1080/000164702321022875
24. Bell WH. Resorption Characteristics of Bone and Bone Substitutes. Oral Surg Oral Med Oral Pathol. 1964;17:650–7.
25. Lillo R, Peltier LF. The substitution of plaster of Paris rods for portions of the diaphysis of the radius in dogs. Surg Forum. 1956;6:556–8.
26. Tay BK, Patel VV, Bradford DS. Calcium sulfate- and calcium phosphate-based bone substitutes. Mimicry Mineral phase bone Orthop Clin North Am. 1999;30:615–23.
27. Kelly CM, Wilkins RM, Gitelis S, Hartjen C, Watson JT, Kim PT. The use of a surgical grade calcium sulfate as a bone graft substitute: results of a multicenter trial. Clin Orthop Relat Res. 2001:42–50. http://graphics.tx.ovid.com/ovftpdfs/FPDDNCJCCBGBCB00/fs046/ovft/live/gv023/00003086/00003086-200101000-00008.pdf.
28. Blaha JD. Calcium sulfate bone-void filler. Orthopedics. 1998;21:1017–9.

29. Calhoun NR, Greene GW Jr., Blackledge GT. Plaster: a bone substitute in the mandible of dogs. J Dent Res. 1965;44:940–6. http://jdr.sagepub.com/content/44/5/940.full.pdf.
30. McKee JC, Bailey BJ. Calcium sulfate as a mandibular implant. Otolaryngol Head Neck Surg. 1984;92:277–86.
31. Walsh WR, Morberg P, Yu Y, et al. Response of a calcium sulfate bone graft substitute in a confined cancellous defect. Clin Orthop Relat Res. 2003;228–36. https://doi.org/10.1097/01.blo.0000030062.92399.6a.
32. Sidqui M, Collin P, Vitte C, Forest N. Osteoblast adherence and resorption activity of isolated osteoclasts on calcium sulphate hemihydrate. Biomaterials. 1995;16:1327–32.
33. Orsini G, Ricci J, Scarano A, et al. Bone-defect healing with calcium-sulfate particles and cement: an experimental study in rabbit. J Biomed Mater Res B Appl Biomater. 2004;68:199–208. https://doi.org/10.1002/jbm.b.20012